N-acetyl-L-cysteine protects rat lungs and RLE-6TN cells from cigarette smoke-induced oxidative stress

JIAMENG CHEN*, YUEFENG CHENG*, HUIJUAN CUI*, SHUANGYAN LI, LANTIAN DUAN and ZONGXIAN JIAO

Department of Pathology, Research Institute of Pathology, School of Basic Medical Sciences, Lanzhou University, Lanzhou, Gansu 730000, P.R. China

Received May 17, 2024; Accepted January 14, 2025

DOI: 10.3892/mmr.2025.13462

Abstract. Cigarette smoke (CS) is a key contributor of chronic obstructive pulmonary disease (COPD); however, its role in the pathogenesis of COPD has not been fully elucidated. N-acetyl-L-cysteine (NAC), as an antioxidant, has been used in the treatment of COPD; however, the mechanisms of action of NAC are not fully understood. Alveolar epithelial type 2 (ATII) cells serve an essential role in the maintenance of alveolar integrity. The aim of the present study was to identify the effect of CS on rat lungs and ATII cells. A subacute lung injury model of Wistar rats was established using CS exposure for 4 weeks. Interalveolar septa widening, infiltration of inflammatory cells, edema fluid in airspaces and abnormal enlargement of airspaces were observed through H&E staining. ELISA revealed that NAC could protect against CS-induced increases in serum levels of malondialdehyde and decreases in serum levels of superoxide dismutase. Additionally, 8-hydroxy-deoxyguanosine was detected using immunohistochemical staining, and this was also expressed at increased levels in the lung tissue of the CS-exposed group. In addition, the expression levels of Bcl-2, BAX and caspase-3 p12 in lung tissue were detected by western blotting or immunohistochemical staining. The expression levels of Bcl-2 decreased and those of caspase3 p12 were increased in response to CS exposure when compared with those in the control group. These effects were prevented by treatment with NAC. *In vitro*, the effect of CS extract (CSE) on rat lung epithelial-6-T-antigen negative (RLE-6TN) cells was observed, flow cytometry was used to detect intracellular reactive oxygen species (ROS) levels and the occurrence of apoptosis, and the content of glutathione (GSH) was detected using a colorimetric assay. Additionally, the expression levels of heme oxygenase-1 (HO-1), p53 and Bcl-2 were examined by western blotting, and HO-1 mRNA expression was also examined using reverse transcription-quantitative PCR. The results of the present study revealed that CSE induced apoptosis of RLE-6TN cells, accompanied by increased levels of intracellular ROS and exhaustion of GSH. Significantly increased protein levels of HO-1 and p53, as well as decreased protein levels of Bcl-2 were also observed. These effects were prevented by administration of NAC. Overall, these findings suggested that CS could promote apoptosis in rat lung tissues and alveolar epithelial cells by inducing intracellular oxidative injury, and NAC may serve an antioxidant role by replenishing the intracellular GSH content.

Correspondence to: Dr Zongxian Jiao, Department of Pathology, Research Institute of Pathology, School of Basic Medical Sciences, Lanzhou University, 222 South Tianshui Road, Lanzhou, Gansu 730000, P.R. China
E-mail: jiaozongx@lzu.edu.cn

*Contributed equally

Key words: chronic obstructive pulmonary disease, N-acetyl-L-cysteine, cigarette smoke, oxidative stress, apoptosis, glutathione

Introduction

Chronic obstructive pulmonary disease (COPD) is the third most common cause of mortality globally and is associated with a high burden of disease (1). The pathogenesis of COPD is complex, involving genetic factors, air pollution and other factors such as oxidative stress, immunologic factors, systemic inflammation, cell senescence, apoptosis and autophagy (2,3). Cigarette smoke (CS) is a preventable cause of COPD (4). It is estimated that 20-25% of smokers eventually develop COPD (5). A single puff of CS is composed of thousands of chemicals, including polycyclic aromatic hydrocarbons (6). Furthermore, it also contains 4,000-7,000 different types of oxidant compounds (7). These oxides and free radicals can elevate the levels of oxidative stress, inactivate the antioxidant defense ability, and cause lung and systemic oxidative stress (8). Through chemical modification of proteins, lipids, carbohydrates and nucleic acids, oxidative distress causes damage to these macromolecules, thereby impairing their function (9).

Oxidative stress is a key factor triggering the occurrence of COPD and its progression, as well as amplifying acute exacerbations (10). Increased oxidative stress in the lungs of patients with COPD leads to chronic inflammation by activating intracellular signaling pathways, reducing anti-inflammatory effects of corticosteroids, accelerating cellular senescence and

lung ageing, inducing autoimmunity based on autoantibodies to carbonylated proteins, and damaging DNA (10,11). Oxidative stress ultimately leads to emphysema by reducing the activity of antiproteases, and promoting extracellular matrix proteolysis, small airway fibrosis and mucus hypersecretion (10). Therefore, antioxidant therapy is a potential approach for the treatment of COPD.

N-acetyl-L-cysteine (NAC) is considered a well-tolerated and safe drug that has been used for decades for the treatment of various medical conditions such as ischemia-reperfusion injury in brain and lethal endotoxemia (12). NAC is a potent antioxidant and is capable of reducing oxidants (13). There are three potential explanations for the mechanism of NAC: i) Breaking disulfide bonds; ii) direct antioxidant activity [scavenging reactive oxygen species (ROS)]; and iii) indirect antioxidant activity [replenishing depleted glutathione (GSH)] (13,14). Although a number of studies have revealed that NAC already has a well-defined mechanism of action (15-17), other studies have revealed that that the mechanism of action of NAC is still unclear and remains to be understood (13,14,18). Thus, the present study aimed to observe the effect of CS in the lungs of rats and rat alveolar epithelial cells by establishing a rat model of COPD and a CS extract (CSE)-induced cell injury model. The present study aimed to determine whether CS could induce oxidative stress in alveolar epithelial cells and in rat lungs and induce apoptosis. The present study also aimed to determine whether NAC could protect against oxidative injury by replenishing depleted intracellular GSH.

Materials and methods

Reagents and antibodies. NAC, 2',7'-dichlorofluorescin diacetate (DCFH-DA) and annexin V-FITC apoptosis detection kits were purchased from Sigma-Aldrich; Merck KGaA. The GSH and GSH disulfide (GSSG) detection kits were purchased from Beyotime Institute of Biotechnology. Cigarettes were purchased from Gansu Tobacco Industrial Co., Ltd. ELISA kits for malondialdehyde (MDA) (cat. no. SP30131) and superoxide dismutase (SOD) (Rat SOD ELISA Kit, SP12914) were purchased from Wuhan Saipei Biotechnology Co., Ltd. The Rabbit Streptavidin-Peroxidase Immunohistochemical staining kit (SP assay kit) and the 3,3-diaminobenzidine (DAB) detection kit were ordered from Beijing Zhongshan Golden Bridge Biotechnology Co., Ltd.

The rabbit anti-8-oxo-7,8-dihydro-2'-deoxyguanosine (8-OHdG) (bs1278R) and rabbit anti-caspase3 p12 (bs0087R) antibodies were purchased from Beijing Biosynthesis Biotechnology Co., Ltd. Other primary antibodies, including heme oxygenase-1 (HO-1) (ab68477), p53 (cat. no. ab26), BAX (ab32503), Bcl-2 (ab59348) and β-actin (ab8227) antibodies, were purchased from Abcam. Other products such as RIPA Lysis Buffer, BCA protein assay kits and phenylmethylsulfonyl fluoride were purchased from Beijing Solarbio Science & Technology Co., Ltd.

Animal models. A total of 32 male 8-week-old Wistar rats weighing ~220 g were purchased from Experimental Animal Center of Lanzhou University (Lanzhou, China). All procedures and animal experiments were carried out in accordance with the protocol approved by the Ethics Committee of the Institutional Animal Care of Lanzhou University (Lzujcyxy20240106; Lanzhou, China). The animals were provided with food and water *ad libitum* and were kept at 22-25˚C and 50-60% relative humidity under a 12-h light/dark cycle. The rats were randomly assigned to the following four groups with eight rats per group: i) Control; ii) CS-exposed group; iii) NAC treatment group; and iv) CS + NAC-exposed group. CS and CS + NAC rats were exposed to CS for 4 weeks using 10 cigarettes twice a day with a 4-6 h interval, 5 days a week. The rats in the NAC group and in the CS+ NAC group were administered NAC dissolved in 0.9% saline solution intragastrically at a dose of 150 $mg/kg^{-1}/day^{-1}$. Body weight was recorded every week. Finally, rats were anesthetized with 1% pentobarbital sodium at a dose of 40 mg/kg by intraperitoneal injection. Subsequently, the rats were sacrificed by exsanguination (~3 ml blood was collected simultaneously) whilst still under anesthesia, and the lungs were removed immediately following euthanasia. Serum was separated by centrifugation at 670 x g for 10 min at 4˚C and stored at -80˚C for biochemical assays. A portion of the lungs was snap-frozen at ~-196˚C in liquid nitrogen for western blotting, while another portion was fixed in 4% paraformaldehyde at room temperature for 24 h for subsequent evaluation of histopathological changes.

ELISA. Serum samples were immediately separated by centrifugation at 670 x g for 10 min at 4˚C. Serum levels of MDA and SOD were detected using highly sensitive rat ELISA kits. The assay was performed according to the manufacturer's instructions, and absorbance was measured at 450 nm using a microplate reader (BIO-RAD680; Bio-Rad Laboratories, Inc.).

H&E staining. Following dehydration with ascending ethanol solution, xylene was used to remove the ethanol, and lung tissues were embedded in paraffin wax and cut into 5-μm-thick sections. These sections were finally stained with hematoxylin and eosin at room temperature for 5 min for histopathological observation under a light microscope (magnification, x100).

Immunohistochemistry. Lung tissues were fixed overnight in 4% paraformaldehyde solution at room temperature, dehydrated using ethanol, embedded in paraffin and sectioned (5 μm) using a microtome. The tissue sections were deparaffinized in xylene and rehydrated using descending concentrations of ethanol solutions (100, 95 and 75% diluted in water). Antigen retrieval was carried out by immersing slides in sodium citrate buffer and heating at 95˚C for 5 min. Slides were then incubated with 3% hydrogen peroxide solution for 10 min and blocked in 10% normal goat serum (Beijing Solarbio Science & Technology Co., Ltd.) for 10-15 min at room temperature. Next, the primary antibodies, 8-OHdG (1:200) and caspase-3 p12 (1:300), were applied to the slides, and slides were incubated overnight at 4˚C, and then rinsed three times for 3 min each in PBS. Subsequently, 100 μl biotin-labeled secondary antibody (SP-9001, Beijing Zhongshan Golden Bridge Biotechnology Co., Ltd.) was applied for 15 min at room temperature and then slides were rinsed three times for 3 min each in PBS. Furthermore, 100 μl horseradish peroxidase-labeled streptavidin (cat. no. ZB-2402, 1:300, Beijing Zhongshan Golden Bridge Biotechnology Co., Ltd.) working solution was incubated at room temperature for

15 min, and then sections were rinsed three times for 3 min each in PBS. DAB was used as a chromogen and the slides were counterstained with hematoxylin for 5 min at room temperature. After dehydration and clearing, the slides were mounted using neutral gum on coverslips. The slides were observed under a light microscope, and images were analyzed using ImageJ software (version 1.52a; National Institutes of Health).

Cell culture and treatment. Rat lung epithelial-6-T-antigen negative (RLE-6TN) cells were purchased from Central South University (Changsha, China) and cultured in Hyclone RPMI 1640 (Cytiva) with 10% fetal bovine serum (Biological Industries; Sartorius AG) at 37˚C in humidified air containing 5% CO_2. CS from three cigarettes was dissolved in 20 ml RPMI 1640. After being adjusted to pH 7.4 and filtered using a 0.22-μm filter to remove bacteria, the solution was regarded as 100% CSE. The cells were then treated with control, 5% CSE and 5% CSE + NAC (1 mM) for 24 h at 37˚C. A solution of 5% CSE was prepared (1:20; 1 part stock solution and 19 parts RPMI 1640 to obtain a total volume of diluted solution equal to 20 times that of the stock solution).

Detection of ROS levels. Measurement of intracellular ROS levels in RLE-6TN cells was based on the ROS-mediated conversion of non-fluorescent DCFH-DA into fluorescent DCF. Briefly, RLE-6TN cells were treated as aforementioned, then washed three times with PBS and incubated in 10 μM DCFH-DA for 30 min at 37˚C in the dark. Cells were harvested by trypsinization, washed again with PBS and resuspended in 1 ml PBS. The fluorescence intensity was measured by flow cytometry (Epics XL; Beckman Coulter, Inc.) and analyzed using FlowJo™ Software v10 (Becton, Dickinson & Company).

GSH assay. To detect the cellular GSH content, GSH and GSSG detection kits (Beyotime Institute of Biotechnology) were used. Briefly, fresh cells were digested with trypsin-EDTA and centrifuged for precipitation at 167 x g for 5 min at 4˚C. Reagent M solution at a volume of three times the pellet was added to remove protein and samples were vortexed vigorously. Next, two rapid freeze-thaws using liquid nitrogen were carried out using a 37˚C water bath. After incubation at 4˚C for 10 min, the samples were centrifuged at 10,000 x g for 10 min at 4˚C. The supernatant was removed and kept at 4˚C for total GSH analysis. Then, 1/5 volume diluted GSH Removal Buffer was added to sample lysate and samples were mixed immediately by vortexing. Subsequently, 1/25 volume GSH removal reagent working solution was added and samples were mixed immediately by vortexing. The mixture was incubated at 25˚C for 60 min and GSH was removed. Reactions were prepared in 96-well plates by mixing samples with 150 μl total GSH assay working solution, which were incubated at room temperature for 5 min. Subsequently, 50 μl of 0.5 mg/ml NADPH solution was added per well and samples were mixed by pipetting. Measurements were performed 25 min after the NADPH solution was added. Based on the A_{412}, total GSH or GSSG content was determined from the standard curve, which was plotted with different concentrations of GSSG. The GSH content was determined by subtracting the GSSG content from the total GSH content as follows: GSH=total GSH-GSSG x2.

Apoptosis analysis. Apoptosis was detected using the annexin V-FITC apoptosis detection kit. Briefly, cells were seeded in a 6-well plate at a density of $1x10^5$ cells/well for 24 h and then the cells were treated as aforementioned. Subsequently, cells were harvested as aforementioned and washed twice with Dulbecco's Phosphate-Buffered Saline). The cells were resuspended in 1X binding buffer at a concentration of $1x10^6$ cells/ml, and 5 μl annexin V-FITC conjugate and 10 μl propidium iodide solution were added to the cell suspension. After a 10-min incubation at room temperature, the cells were analyzed by flow cytometry (Epics XL; Beckman Coulter, Inc.) and analyzed using FlowJo™ Software v10 (Becton, Dickinson & Company).

Western blotting. Total protein from lung tissue or RLE-6TN cells was isolated using RIPA Lysis Buffer with 1% protease inhibitor. The protein concentration of each group was determined using BCA protein assay kits. The samples were separated by 12% SDS-PAGE loaded as 40 μg/ml per lane and transferred to a methanol-activated PVDF membrane. The membrane was blocked with 5% BSA (Beijing Solarbio Science & Technology Co., Ltd) in TBS with 0.1% Tween 20 (TBST) for 1.5 h at room temperature and subsequently incubated with primary antibodies overnight at 4˚C. The primary antibodies were: HO-1 (1:10,000; Abcam), anti-p53 (1:200; Abcam), anti-Bcl2 (1:500; Abcam), anti-Bax (1:1,000; Abcam), anti-β-actin (1:5,000; Abcam), anti-β-tubulin (1:5,000; Abcam) and anti-GAPDH (1:10,000; ImmunoWay Biotechnology Company). Membranes were washed three times for 8 min each with TBST, incubated with DyLight 800 Labeled secondary antibody (1:5,000, KPL, Inc.) at room temperature for 1.5 h, washed three times for 8 min each and bands were detected using an Odyssey Infrared Imaging System (LI-COR Biosciences) and analyzed with ImageJ software version 1.50i (National Institutes of Health, Bethesda, Maryland, USA).

Reverse transcription-quantitative PCR (RT-qPCR). Total RNA was isolated from RLE-6TN cells using RNAiso Plus (Takara Bio, Inc.) and reverse transcription was carried out using a PrimeScript™ RT reagent Kit with gDNA Eraser (Takara Bio, Inc.) according to the manufacturer's instructions. qPCR was conducted using TB Green® Premix Ex Taq II (Takara Bio, Inc.). The thermocycling conditions were as follows: Initial denaturation at 95˚C for 30 sec, followed by 50 cycles of 95˚C for 5 sec and 60˚C for 34 sec. β-actin was used as the internal control and the expression levels of the target gene were calculated using the $2^{-\Delta\Delta Cq}$ method (19). The primers used were: β-actin forward, 5'-GGAGATTACTGC CCTGGCTCCTA-3' and reverse, 5'-GACTCATCGTACTCC TGCTTGCTG-3'; and HO-1 forward, 5'-AGGTGCACATCC GTGCAGAG-3' and reverse, 5'-CTTCCAGGGCCGTATAGA TATGGTA-3'.

Statistical analysis. Statistical analysis was carried out using SPSS (version 22; IBM Corp.). The experimental data are presented as the mean ± SD of ≥3 independent experiments. Statistical significance was determined using one-way analysis of variance and comparisons among groups were performed using Fisher's Least Significant Difference test or the

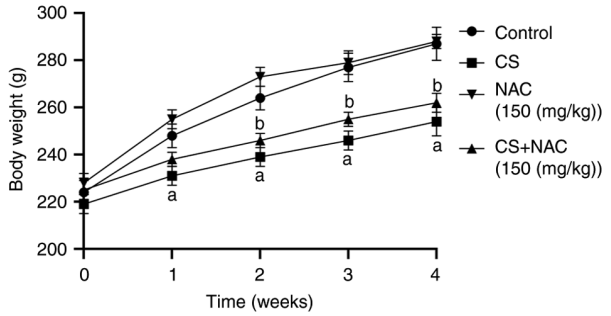

Figure 1. Body weight (g) changes of Wistar rats after treatment with CS and/or NAC for 4 weeks. [a]P<0.01 vs. control group; [b]P<0.05 vs. CS group. CS, cigarette smoke; NAC, N-acetyl-L-cysteine.

Bonferroni test. P<0.05 was considered to indicate a statistically significant difference.

Results

Body weight changes of Wistar rats during the experimental procedure. The body weight of the rats is shown in Fig. 1. The initial body weight was not significantly different among the three groups. Rats treated with normal saline exhibited the highest body weight gain. The weight of the CS group was decreased compared with that of the control group at each week (P<0.01). Compared with the CS group, the CS + NAC group exhibited an increase in body weight from the end of week 2 to week 4 (P<0.05). These results indicated that NAC intake may protect rats from CS-induced weight reduction.

Histopathological alterations of rat lung tissue exposed to CSE. H&E staining results are presented in Fig. 2. The structures of the lung tissues were normal in the control group. By contrast, the lung tissues of rats exposed to CS exhibited interalveolar septa widening, infiltration of inflammatory cells, edema fluid in airspaces and abnormal enlargement of airspaces. These characteristics were attenuated in the CS + NAC group. These results indicated that NAC could protect rat lungs from CS-induced injury.

CS-induced oxidative stress in rats. MDA is a classic representative of lipid peroxidation products and 8-OHdG is a marker of DNA damage; these reflect the levels of oxidative stress (20). SOD is an antioxidant enzyme, which mitigates oxidative stress (21). Therefore, the effects of CS + NAC on oxidative stress were examined by measuring MDA and SOD levels in the serum, and 8-OHdG levels in lung tissues. The results shown in Fig. 3 indicated increased levels of MDA and decreased levels of SOD in the serum of Wistar rats exposed to CS compared with the control group (P<0.05). NAC treatment significantly prevented these changes compared with the CS group (P<0.05). The immunohistochemistry results revealed that the positive expression of 8-OHdG in CS-exposed rat lungs was increased compared with that in the control group; however, this was decreased following simultaneous administration of NAC. These results indicated that CS stimulated changes in the expression of oxidative stress-related markers, and that NAC effectively antagonized the oxidative injury.

Effects of NAC on CS-induced apoptosis in rat lungs. Although there was no significant change in the expression levels of BAX in the lungs of CS-exposed rats compared with the control group, Bcl-2 expression was significantly decreased compared with that in the control group (P<0.05). Additionally, the CS + NAC group exhibited increased expression levels of Bcl-2 compared with the CS-exposed group (P<0.05). Correspondingly, the results of immunohistochemical staining revealed that the expression levels of Caspase-3 p12 in lung tissue were increased following CS exposure, and this was antagonized by the administration of NAC. Therefore, CS may stimulate apoptosis in lung tissue, whereas NAC may protect against apoptosis (Fig. 4).

Effects of NAC on CSE-induced oxidative stress in RLE-6TN cells. After incubation of RLE-6TN cells with DCFH-DA, intracellular ROS levels were detected. Compared with those in the control group, CSE significantly increased the average fluorescence intensity as well as the percentage of fluorescent cells in the CSE group. Co-treatment with NAC resulted in a significant decrease in these parameters compared with the CSE group (Figs. 5A and B, S1 and S2). HO-1 mRNA and protein expression under CSE stimulation was subsequently investigated. Analysis revealed that both mRNA and protein levels of HO-1 were significantly upregulated by CSE compared with the control group. Co-treatment with NAC significantly prevented the induction of HO-1 compared with the CSE group (Fig. 5C and D). The upregulation of HO-1 in CSE-treated cells may be in response to CSE-induced oxidative stress, since HO-1 is an antioxidant.

GSH content alterations in RLE-6TN cells by CSE and/or NAC. The concentration of GSH in the 5% CSE-treated group was reduced compared with that in the control group (P<0.05; Fig. 6). Co-treatment with NAC resulted in increased levels of GSH compared with the CSE-treated group (P<0.05). In summary, CSE-induced oxidative stress could oxidize or exhaust intracellular GSH, and NAC may protect alveolar epithelial cells by replenishing the lost GSH.

Effects of NAC on CSE-induced apoptosis in RLE-6TN cells. p53 expression was upregulated in alveolar epithelial cells following 5% CSE administration (Fig. 7A), and correspondingly anti-apoptotic protein Bcl2 was significantly downregulated (Fig. 7B) compared with the control group; however, the expression levels of the pro-apoptotic protein BAX did not change (Fig. S3). At the same time, co-treatment with NAC could prevent the aforementioned alterations. As shown by flow cytometry analysis (Fig. 7C), in the control group, the percentage of cells in Q2 + Q3 was 13.43%. In cells exposed to 5% CSE, this increased to 66.6%. In CSE-treated RLE-6TN cells co-treated with NAC, the percentage of cells in Q2 + Q3 decreased to 35.2%. These data indicated that CSE may induce apoptosis of alveolar epithelial cells, while NAC prevented CSE-induced oxidative injury.

Discussion

COPD is a global health problem that is increasing in incidence and mortality. It is estimated that the global prevalence

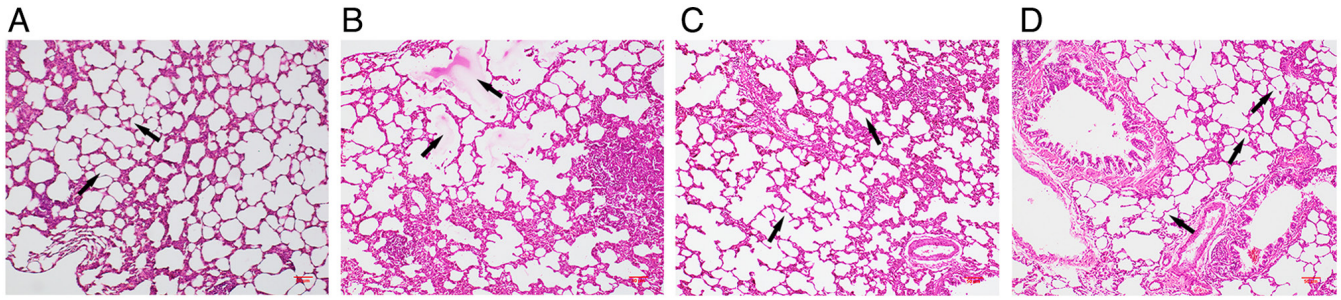

Figure 2. Effects of NAC on CS-induced morphological changes of lung tissue (H&E staining; magnification, x100; scale bar, 50 μm). (A) Control. (B) CS group. (C) NAC group. (D) CS + NAC group. Black arrows indicate structures of interalveolar septa and alveolar space. CS, cigarette smoke; NAC, N-acetyl-L-cysteine.

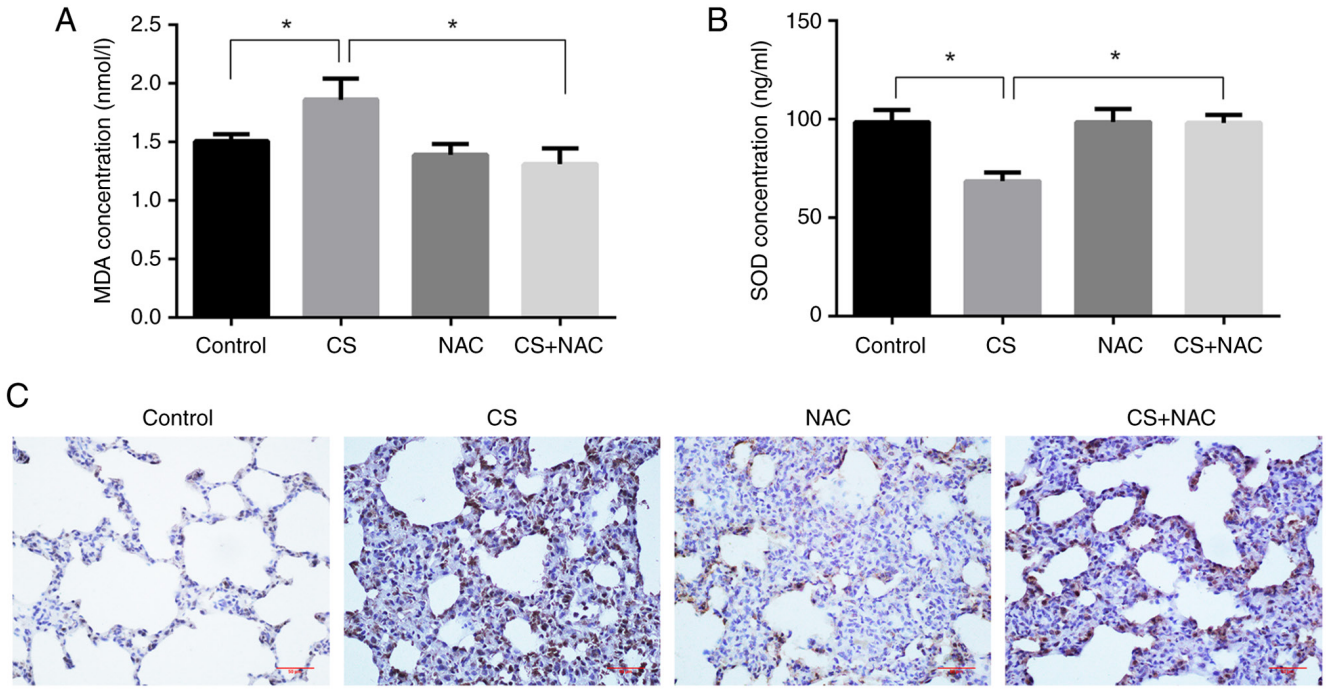

Figure 3. Effects of NAC on CS-induced oxidative stress. Serum levels of (A) MDA and (B) SOD. (C) Expression levels of 8-hydroxy-deoxyguanosine in lung tissues of rats (magnification, x100; scale bar, 50 μm) in the Con, CS, NAC and CS + NAC groups. Data are presented as the mean ± SD (n=3). *P<0.05. Con, control; CS, cigarette smoke; MDA, malondialdehyde; NAC, N-acetyl-L-cysteine; SOD, superoxide dismutase.

is 9-10% in adults >40 years (22). CS is an important preventable risk factor for human health, not only for smokers, but also for non-smokers who bear tobacco-associated disease (23), accounting for ~27% of tobacco-related mortalities in smokers and non-smokers (24).

To induce emphysema-like changes and airway remodeling, animals are exposed to CS for at least several days (25). In the present study, Wistar rats were exposed to CS for 4 weeks, and using H&E staining, the presence of characteristics such as airspace enlargement, chronic inflammation and airway remodeling, including interalveolar septa widening, was observed. The presence of these characteristics was attenuated when NAC was simultaneously applied alongside CS exposure.

COPD is considered to be a disease that involves multiple systems, including skeletal muscle wasting, muscle dysfunction and weight loss (26). Nicotine can induce a decrease in appetite, impacting food intake and body weight by influencing the hypothalamic melanocortin system (27). CS contains ≥6,000 components that may directly or indirectly affect energy expenditure (28), and in a subchronic cigarette exposure model of mice, it has been reported that 4-week CS exposure could markedly decrease body weight, food intake, fat mass and the plasma leptin concentration by fundamentally altering hypothalamic appetite regulation in the central nervous system (27). Consistently, the results of the present study revealed that the body weight of rats in the CS group was significantly decreased compared with that in the control group at each week. Co-treatment with NAC resulted in a trend of increased body weight from the end of week 2 until week 4 compared with the CS group.

MDA and 4-hydroxynonenal are biomarkers of lipid peroxidation, and oxidative damage to DNA focuses on oxidation of guanine to 8-OHdG (29). Therefore, the relative contents of SOD, MDA and 8-OHdG are often used as markers of oxidative stress in various lung diseases (11). In the present study, the

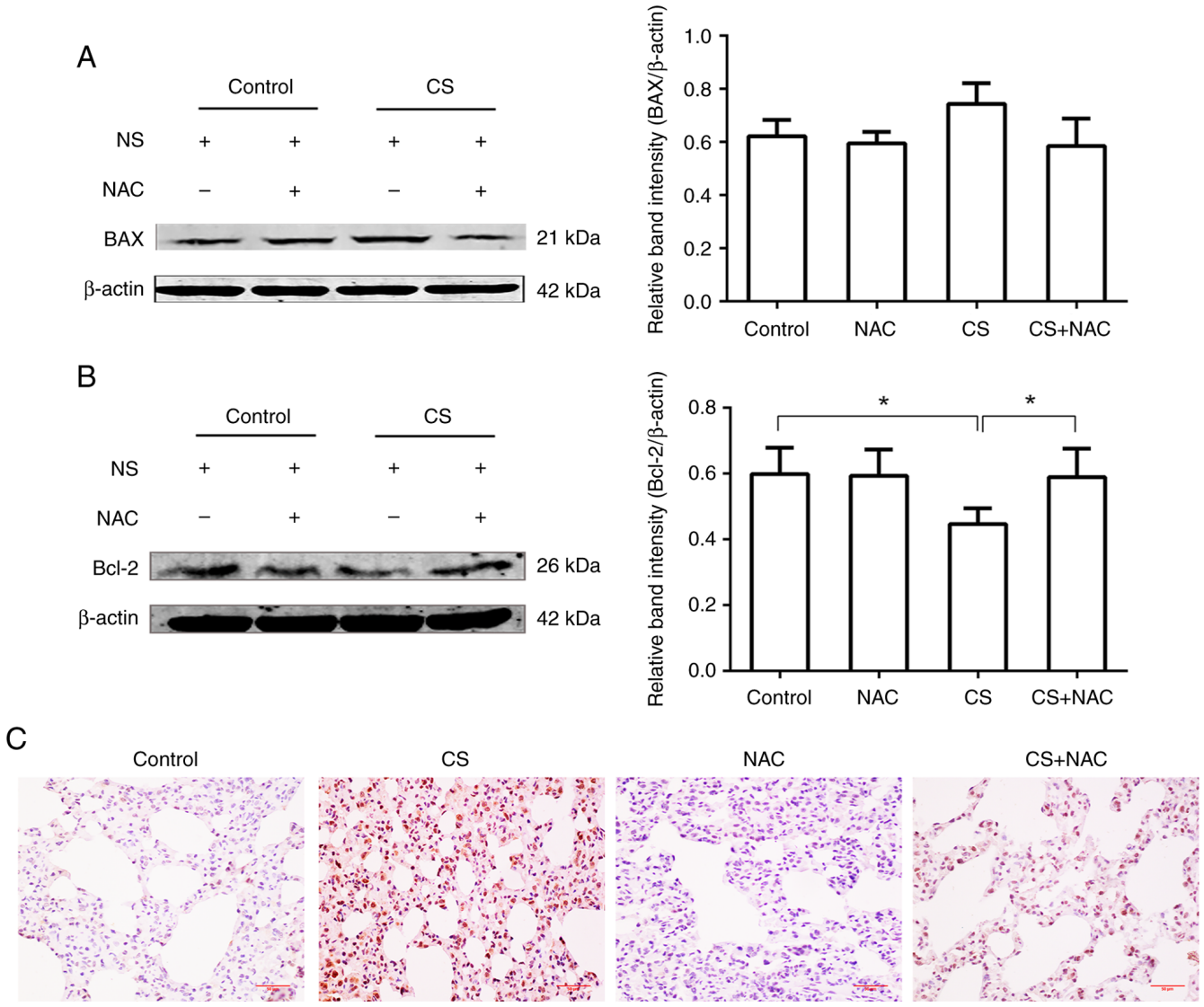

Figure 4. Effect of NAC on CS-induced apoptosis. Expression levels of (A) BAX, (B) Bcl-2 and (C) caspase-3 p12 in lung tissues of rats (immunohistochemical staining; magnification, x100; scale bar, 50 μm) in the Con, CS, NAC and CS + NAC groups. Data are presented as the mean ± SD (n=3). *P<0.05. Con, control; CS, cigarette smoke; NAC, N-acetyl-L-cysteine; NS, normal saline.

content of SOD in serum was significantly decreased, while MDA content in the serum and 8-OHdG content in lung tissue were increased in the CS group. Furthermore, Bcl-2 expression was significantly decreased, while caspase-3 p12 expression was increased in the CS group compared with the control group. Under normal conditions, caspase-3 has no activity and is stored in the form of a zymogen in the cytoplasm; however, when activated by upstream caspases, caspase-3 generates activated caspase-3 p17 and caspase-3 p12 subunits, which serve a role in apoptosis (30). The results indicated that CS could induce oxidative stress and apoptosis in the rat lungs. Co-treatment with NAC prevented the aforementioned changes, suggesting that NAC may protect against CS-induced oxidative damage.

The alveolar epithelium is the initial defense against inhaled particles and gases, as a progenitor for new alveolar epithelial type 1 (ATI) and alveolar epithelial type 2 (ATII) cells during lung repair (31). Following injury of ATI cells, adjacent ATII cells are stimulated to multiply and transdifferentiate into ATI cells (32). In order to study the contribution of ATII cells in the pathogenesis of COPD, the changes in RLE-6TN cells under the stimulation of CSE were observed *in vitro*. The results revealed that CSE induced apoptosis of RLE-6TN cells, produced high levels of intracellular ROS, increased HO-1 expression and exhausted GSH. It also increased p53 expression and decreased Bcl-2 expression. *In vitro* study confirmed that CSE could initiate oxidative stress in RLE-6TN cells and induce apoptosis of alveolar epithelial cells by increasing p53 expression, while decreasing Bcl-2 expression, and NAC could antagonize these changes.

An increase in oxidative stress of alveolar epithelial cells can lead to decrease of intracellular GSH by transversion of GSH to GSSG (33), and the inhibitory effect of NAC suggests that oxidative stress serves an important role in mediating the injury of alveolar epithelial cells by CSE. NAC has been shown to reduce oxidative stress by both direct antioxidant effects, as free sulfydryl groups serve as a source of reducing equivalents, and by indirect antioxidant effects through the replenishment

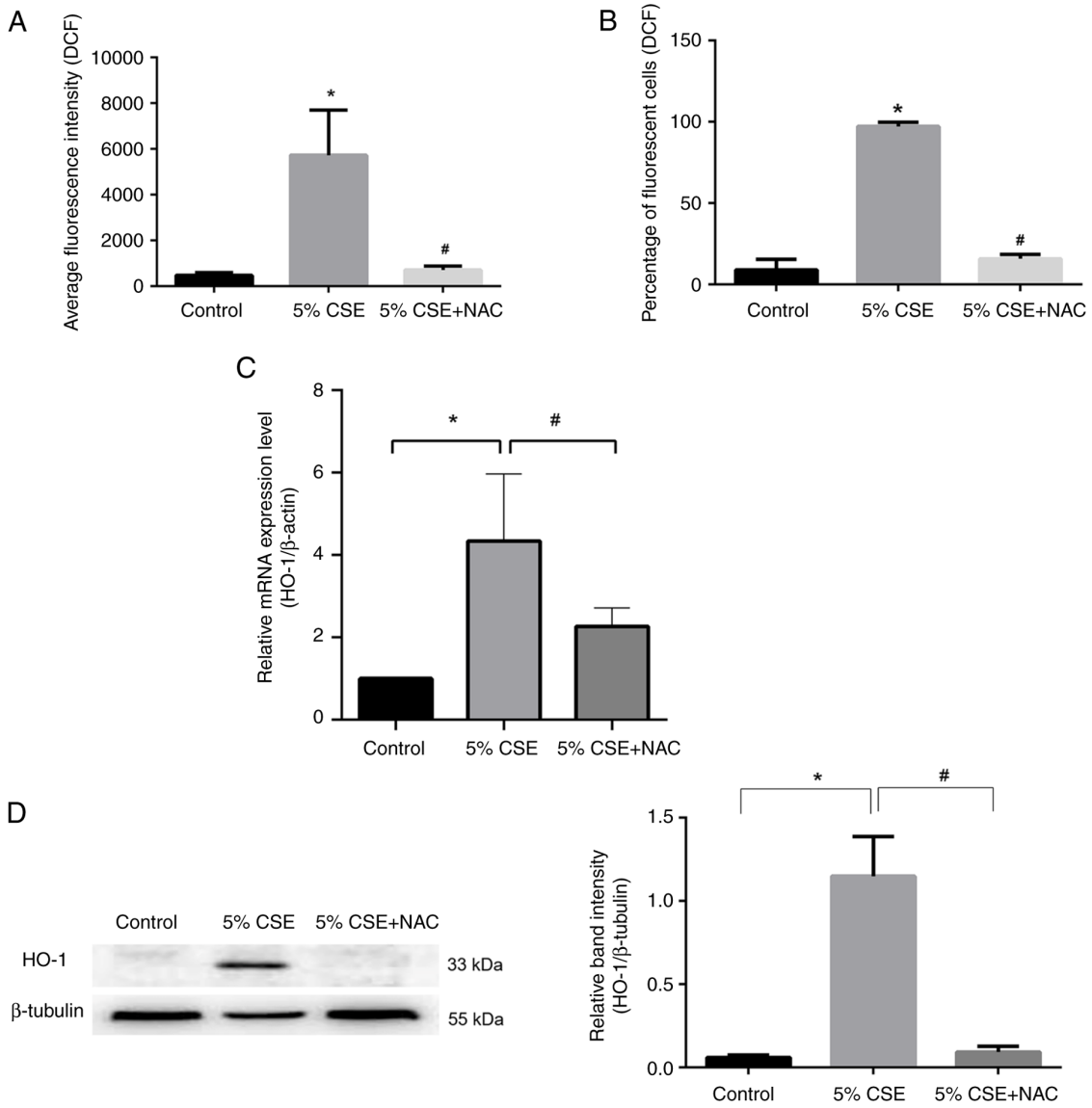

Figure 5. Effects of NAC on CSE-induced oxidative stress. (A) Average fluorescence intensity of DCF in RLE-6TN cells and (B) average percentages of fluorescent cells in the control, CSE and CSE + NAC groups. (C) HO-1 mRNA expression in RLE-6TN cells in the control, CSE or CSE + NAC groups. (D) HO-1 expression in RLE-6TN cells in the control, CSE or CSE + NAC groups. Data are presented as the mean ± SD (n=3). *P<0.05 vs. control group; #P<0.05 vs. 5% CSE group. CSE, cigarette smoke extract; CON, control; DCF, 2'-7'dichlorofluorescein; HO-1, heme oxygenase-1; NAC, N-acetyl-L-cysteine; RLE-6TN, rat lung epithelial-6-T-antigen negative.

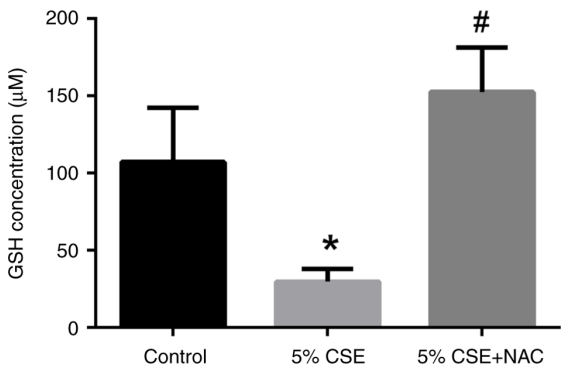

Figure 6. Intracellular GSH content. The GSH concentration in rat lung epithelial-6-T-antigen negative cells was calculated and was significantly decreased by CSE-induced oxidative stress; however, it was increased following treatment with NAC. Data are presented as the mean ± SD (n=3). *P<0.05 vs. control group; #P<0.05 vs. 5% CSE group. CSE, cigarette smoke extract; GSH, glutathione; NAC, N-acetyl-L-cysteine.

of intracellular GSH levels (18). Studies suggest that NAC acts as a donor of sulfane sulfur when provided to cells (14,34), which may form dependently or independently of H_2S, and is likely to exert a cytoprotective effect independently of GSH replenishment. This may occur by modulation of protein activity, protection of thiols from irreversible modifications and/or increased oxidant scavenging capacity (14).

Concomitant with the decrease in GSH, the presence of cellular oxidative stress in CSE-treated cells was also evidenced by the induction of HO-1, which supports the hypothesis that CSE induction of HO-1 is regulated by changes in intracellular GSH. As a precursor of GSH, NAC could significantly reduce the expression of HO-1 stimulated by CSE. HO enzymes catalyze heme to form equimolar amounts of ferrous iron, carbon monoxide and biliverdin, all of which have cytoprotective properties, probably by mitigating nitrosative/oxidative stress (35). Under basal

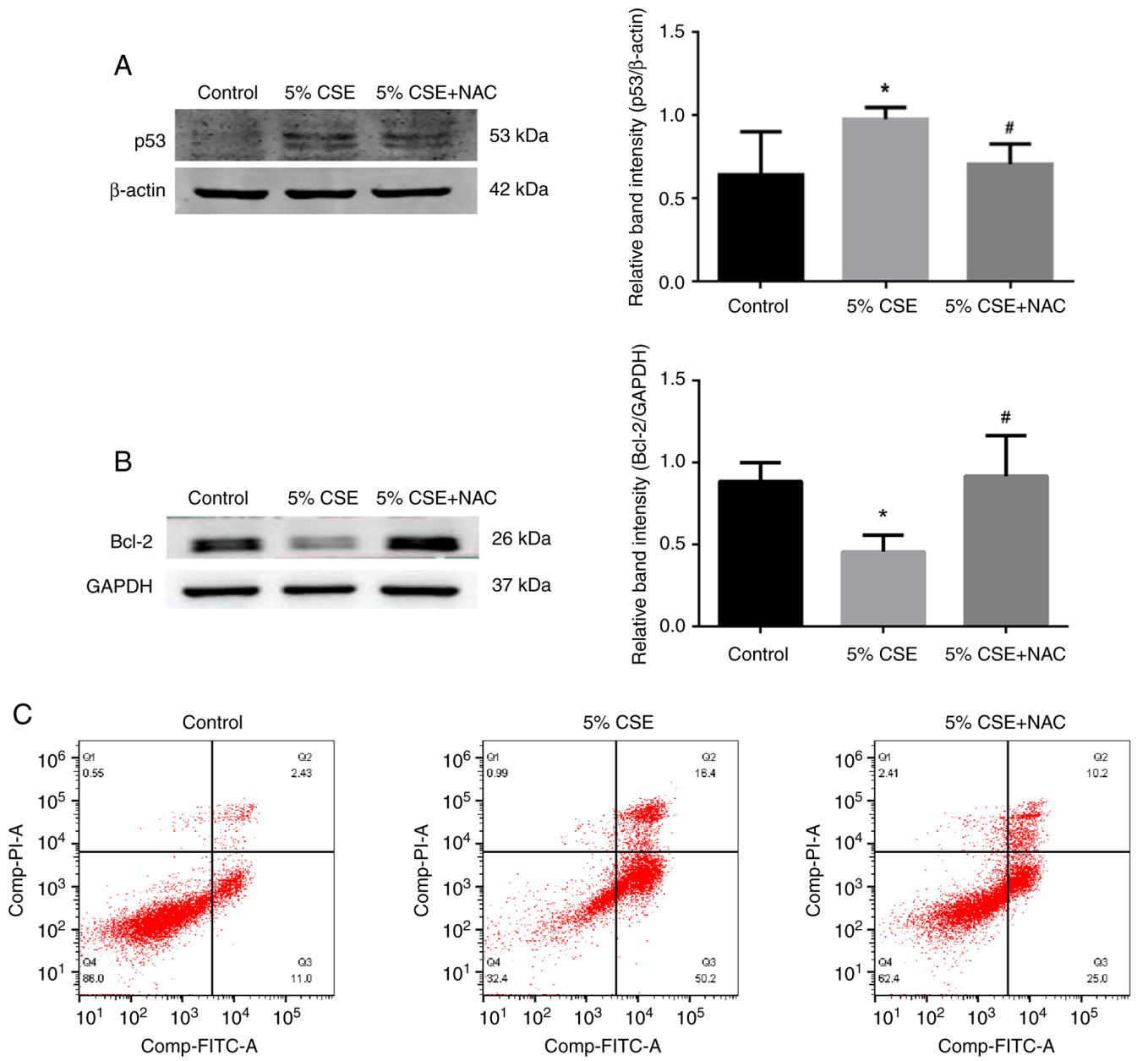

Figure 7. Effects of NAC on CSE-induced apoptosis. (A) p53 protein expression in RLE-6TN cells was upregulated by CSE stimulation; however, NAC could prevent the upregulation. (B) Protein expression levels of Bcl-2, an anti-apoptotic protein, in RLE-6TN cells were downregulated in the CSE-induced group; however, NAC could prevent the downregulation. Data are presented as the mean ± SD (n=3). *P<0.05 vs. control group; $^{\#}$P<0.05 vs. 5% CSE group. (C) Flow cytometry analysis of apoptosis. Q1 represents annexin V^{-}/PI^{+} cells, Q2 represents annexin V^{+}/PI^{+} cells, Q3 represents annexin V^{+}/PI^{-} cells and Q4 represents annexin V^{-}/PI^{-} cells. In the control group, the cell percentage in Q2 + Q3 was 13.43%. Upon exposure to 5% CSE for 24 h, it was increased to 66.6%. By contrast, following co-treatment with NAC, the proportion was decreased to 35.2%. These data indicated that NAC could antagonize the apoptosis induced by CSE. Representative plots of at least three independent experiments are shown. CSE, cigarette smoke extract; NAC, N-acetyl-L-cysteine; RLE-6TN, rat lung epithelial-6-T-antigen negative.

conditions, HO-1 is present at low to undetectable levels in most tissues, but its expression is rapidly increased in response to environmental stimuli producing oxidative stress and generating ROS, thus rapid elevation in HO-1 expression as a response to oxidative stress is usually considered to be a cellular defense mechanism (36). Although modest HO-1 expression is cytoprotective, exacerbation of oxidative injury is often associated with increased HO-1 expression, and increasing evidence suggests that HO-1 induction can also lead to cell injury, presumably through excessive ROS generation (37-39). It is hypothesized that both excess HO activation and iron accumulation generate ROS, and free iron-mediated Fenton reactions have been implicated in lipid peroxidation during ferroptosis in the pathogenesis of COPD (40).

In summary, CS could cause systemic (serum) and local (lung tissue) oxidative stress and ultimately caused apoptosis in lung tissues as well as ATII cells *in vitro*. The protective effects of NAC on alveolar epithelial cells injured by CS may be partially associated with the replenishment of intracellular GSH. These results provide fundamental support for the clinical application of NAC in the treatment of patients with COPD.

Acknowledgements

Not applicable.

Funding

The present study was supported by the National Natural Science Foundation of China (grant no. 81770044).

Availability of data and materials

The data generated in the present study may be requested from the corresponding author.

Authors' contributions

ZJ designed the project. HC carried out the animal experiments. YC, JC and LD carried out the *in vitro* experiments, including mainly western blotting. SL carried out the flow cytometry experiments. JC carried out statistical analysis and drew the histograms. ZJ organized all data and wrote the manuscript. All authors have read and approved the final manuscript. ZJ and JC confirm the authenticity of all the raw data.

Ethics approval and consent to participate

Animal procedures were approved by the Ethics Committee of the Institutional Animal Care of Lanzhou University (approval no. Lzujcyxy20240106; Lanzhou, China).

Patient consent for publication

Not applicable.

Competing interests

The authors declare that they have no competing interests.

References

1. Kahnert K, Jörres RA, Behr J and Welte T: The diagnosis and treatment of COPD and its comorbidities. Dtsch Arztebl Int 120: 434-444, 2023.
2. Song Q, Chen P and Liu XM: The role of cigarette smoke-induced pulmonary vascular endothelial cell apoptosis in COPD. Respir Res 22: 39, 2021.
3. Devulder JV: Unveiling mechanisms of lung aging in COPD: A promising target for therapeutics development. Chin Med J Pulm Crit Care Med 2: 133-141, 2024.
4. Kaur M, Chandel J, Malik J and Naura AS: Particulate matter in COPD pathogenesis: An overview. Inflamm Res 71: 797-815, 2022.
5. Chen L, Zhu D, Huang J, Zhang H, Zhou G and Zhong X: Identification of hub genes associated with COPD through integrated bioinformatics analysis. Int J Chron Obstruct Pulmon Dis 17: 439-456, 2022.
6. Prieux R, Eeman M, Rothen-Rutishauser B and Valacchi G: Mimicking cigarette smoke exposure to assess cutaneous toxicity. Toxicol In Vitro 62: 104664, 2020.
7. Fischer BM, Voynow JA and Ghio AJ: COPD: Balancing oxidants and antioxidants. Int J Chron Obstruct Pulmon Dis 10: 261-276, 2015.
8. Woźniak A, Górecki D, Szpinda M, Mila-Kierzenkowska C and Woźniak B: Oxidant-antioxidant balance in the blood of patients with chronic obstructive pulmonary disease after smoking cessation. Oxid Med Cell Longev 2013: 897075, 2013.
9. Sies H and Jones DP: Reactive oxygen species (ROS) as pleiotropic physiological signalling agents. Nat Rev Mol Cell Biol 21: 363-383, 2020.
10. Barnes PJ: Oxidative stress in chronic obstructive pulmonary disease. Antioxidants (Basel) 11: 965, 2022.
11. Cha SR, Jang J, Park SM, Ryu SM, Cho SJ and Yang SR: Cigarette smoke-induced respiratory response: Insights into cellular processes and biomarkers. Antioxidants (Basel) 12: 1210, 2023.
12. Paintlia MK, Paintlia AS, Contreras MA, Singh I and Singh AK: Lipopolysaccharide-induced peroxisomal dysfunction exacerbates cerebral white matter injury: Attenuation by N-acetyl cysteine. Exp Neurol 210: 560-576, 2008.
13. Aldini G, Altomare A, Baron G, Vistoli G, Carini M, Borsani L and Sergio F: N-Acetylcysteine as an antioxidant and disulphide breaking agent: The reasons why. Free Radic Res 52: 751-762, 2018.
14. Pedre B, Barayeu U, Ezerina D and Dick TP: The mechanism of action of N-acetylcysteine (NAC): The emerging role of H(2)S and sulfane sulfur species. Pharmacol Ther 228: 107916, 2021.
15. Millea PJ: N-acetylcysteine: Multiple clinical applications. Am Fam Physician 80: 265-269, 2009.
16. Sanguinetti CM: N-acetylcysteine in COPD: Why, how, and when? Multidiscip Respir Med 11: 8, 2016.
17. Messier EM, Day BJ, Bahmed K, Kleeberger SR, Tuder RM, Bowler RP, Chu HW, Mason RJ and Kosmider B: N-Acetylcysteine protects murine alveolar type II cells from cigarette smoke injury in a nuclear erythroid 2-related factor-2-independent manner. Am J Respir Cell Mol Biol 48: 559-567, 2013.
18. Cazzola M, Page CP, Wedzicha JA, Celli BR, Anzueto A and Matera MG: Use of thiols and implications for the use of inhaled corticosteroids in the presence of oxidative stress in COPD. Respir Res 24: 194, 2023.
19. Burkhardt BR, Lyle R, Qian K, Arnold AS, Cheng H, Atkinson MA and Zhang YC: Efficient delivery of siRNA into cytokine-stimulated insulinoma cells silences Fas expression and inhibits Fas-mediated apoptosis. FEBS Lett 580: 553-560, 2006.
20. Murphy MP, Bayir H, Belousov V, Chang CJ, Davies KJA, Davies MJ, Dick TP, Finkel T, Forman HJ and Janssen-Heininger Y, *et al*: Guidelines for measuring reactive oxygen species and oxidative damage in cells and in vivo. Nat Metab 4: 651-662, 2022.
21. Dang X, He B, Ning Q, Liu Y, Guo J, Niu G and Chen M: Alantolactone suppresses inflammation, apoptosis and oxidative stress in cigarette smoke-induced human bronchial epithelial cells through activation of Nrf2/HO-1 and inhibition of the NF-κB pathways. Respir Res 21: 95, 2020.
22. Vijayan VK: Chronic obstructive pulmonary disease. Indian J Med Res 137: 251-269, 2013.
23. Salvi SS and Barnes PJ: Chronic obstructive pulmonary disease in non-smokers. Lancet 374: 733-743, 2009.
24. Martinez FJ, Donohue JF and Rennard SI: The future of chronic obstructive pulmonary disease treatment-difficulties of and barriers to drug development. Lancet 378: 1027-1037, 2011.
25. Upadhyay P, Wu CW, Pham A, Zeki AA, Royer CM, Kodavanti UP, Takeuchi M, Bayram H and Pinkerton KE: Animal models and mechanisms of tobacco smoke-induced chronic obstructive pulmonary disease (COPD). J Toxicol Environ Health B Crit Rev 26: 275-305, 2023.
26. Henrot P, Blervaque L, Dupin I, Zysman M, Esteves P, Gouzi F, Hayot M, Pomiès P and Berger P: Cellular interplay in skeletal muscle regeneration and wasting: Insights from animal models. J Cachexia Sarcopenia Muscle 14: 745-757, 2023.
27. Mineur YS, Abizaid A, Rao Y, Salas R, DiLeone RJ, Gündisch D, Diano S, De Biasi M, Horvath TL, Gao XB and Picciotto MR: Nicotine decreases food intake through activation of POMC neurons. Science 332: 1330-1332, 2011.
28. Chen H, Hansen MJ, Jones JE, Vlahos R, Bozinovski S, Anderson GP and Morris MJ: Cigarette smoke exposure reprograms the hypothalamic neuropeptide Y axis to promote weight loss. Am J Respir Crit Care Med 173: 1248-1254, 2006.
29. Jomova K, Raptova R, Alomar SY, Alwasel SH, Nepovimova E, Kuca K and Valko M: Reactive oxygen species, toxicity, oxidative stress, and antioxidants: Chronic diseases and aging. Arch Toxicol 97: 2499-2574, 2023.

30. Boatright KM and Salvesen GS: Caspase activation. Biochem Soc Symp 233-242, 2003.
31. Ruaro B, Salton F, Braga L, Wade B, Confalonieri P, Volpe MC, Baratella E, Maiocchi S and Confalonieri M: The history and mystery of alveolar epithelial type II cells: Focus on their physiologic and pathologic role in lung. Int J Mol Sci 22: 2566, 2021.
32. Han S, Lee M, Shin Y, Giovanni R, Chakrabarty RP, Herrerias MM, Dada LA, Flozak AS, Reyfman PA, Khuder B, *et al*: Mitochondrial integrated stress response controls lung epithelial cell fate. Nature 620: 890-897, 2023.
33. Baglole CJ, Bushinsky SM, Garcia TM, Kode A, Rahman I, Sime PJ and Phipps RP: Differential induction of apoptosis by cigarette smoke extract in primary human lung fibroblast strains: Implications for emphysema. Am J Physiol Lung Cell Mol Physiol 291: L19-L29, 2006.
34. Ezeriņa D, Takano Y, Hanaoka K, Urano Y and Dick TP: N-Acetyl cysteine functions as a fast-acting antioxidant by triggering intracellular H(2)S and sulfane sulfur production. Cell Chem Biol 25: 447-459.e4, 2018.
35. Wu CY, Cilic A, Pak O, Dartsch RC, Wilhelm J, Wujak M, Lo K, Brosien M, Zhang R, Alkoudmani I, *et al*: CEACAM6 as a novel therapeutic target to boost HO-1-mediated antioxidant defense in COPD. Am J Respir Crit Care Med 207: 1576-1590, 2023.
36. Consoli V, Sorrenti V, Grosso S and Vanella L: Heme oxygenase-1 signaling and redox homeostasis in physiopathological conditions. Biomolecules 11: 589, 2021.
37. Lee DW, Gelein RM and Opanashuk LA: Heme-oxygenase-1 promotes polychlorinated biphenyl mixture aroclor 1254-induced oxidative stress and dopaminergic cell injury. Toxicol Sci 90: 159-167, 2006.
38. Lin CC, Yang CC, Hsiao LD, Chen SY and Yang CM: Heme oxygenase-1 induction by carbon monoxide releasing molecule-3 suppresses interleukin-1β-mediated neuroinflammation. Front Mol Neurosci 10: 387, 2017.
39. Baglole CJ, Sime PJ and Phipps RP: Cigarette smoke-induced expression of heme oxygenase-1 in human lung fibroblasts is regulated by intracellular glutathione. Am J Physiol Lung Cell Mol Physiol 295: L624-L636, 2008.
40. Jiang X, Stockwell BR and Conrad M: Ferroptosis: Mechanisms, biology and role in disease. Nat Rev Mol Cell Biol 22: 266-282, 2021.